Controller for surface plasmons resonance based biosensor using Reconfigurable Computing and Virtual Instruments.

Leiva C. Oliveira [1], *Luiz C.P. Grilo* [2], *A.M.N. Lima*[3] *e Elmar. K. U. Melcher* [4]

[1,4] Departamento de Sistemas de Computação
[1,2,3] Departamento de Engenharia Elétrica
Universidade Federal de Campina Grande
Rua Aprígio Veloso, 882, 58429-900 - Caixa Postal 10.105, Campina Grande, Paraíba – BR
e-mail: leiva.oliveira@ee.ufcg.edu.br, amnlima@ee.ufcg.edu.br

Abstract: A controller for surface plasmon resonance biosensor has been designed and applied for analysis of aqueous substances. A core provides the necessary signals for control and sensor actuation. Using a 16 bits A/D converter to convert the analog signals generated by the sensor and polynomial algorithm, the sensor output noise are reduced around 37.5%. The digital data are sent to computer for processed and displayed. Details regarding the physics construction of the controller and its programming, including system validation tests presented in this paper.

Key words: Biosensor SPR, Virtual Instruments, Reconfigurable Computing, FPGA.

1. INTRODUCTION

The surface plasmons resonance (SPR) based biosensor technology consists in biochemical-electronic devices capable of identifying, process and quantify a biological event, usually through electrical or optical signals. These devices replaced conventional methods due the fast response, high sensitivity, versatility and label-free measurements [1,5]. Basically, SPR biosensors integrate an optical apparatus with a microfluidic system. The typical SPR biosensor set-up is shown in Figure 1. It comprises a four layer configuration [5]: (1) an optical coupling substrate (prism, waveguide, optical fiber, diffraction grating), (2) a thin metal film (use of noble metals particularly gold), (3) a bio-recognition coating which interacts with target molecules present in (4) the fluidic sample that enters through flow cell. Due the bio-recognition surface can be "prepared" for many different purposes, SPR biosensors gives flexibility in your niche of expertise, enabling them to detect pathogens [3], determine biomolecular interactions [2] and detecting contaminants in food for quality control [4].

Among the SPR biosensors commercial systems, Spreeta™ Evaluation Kit [6] has one of the lowest market prices. However, its interface controller has a low resolution in electrical signals conversion (8 bits) resulting in an noise increase associated with refractive index detection.

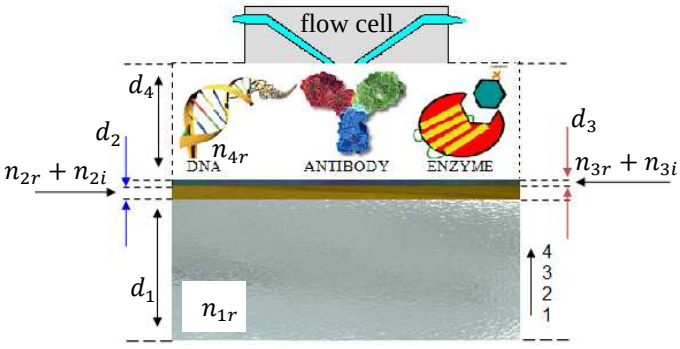

Fig. 1. Multilayer SPR biosensor structure. Layers are numbered bottom to top.

Here we present an interface that is responsible for managing the SPR sensor Spreeta, marketed by Texas Instruments (TI). Developed using reconfigurable computing, its functions are the correct signals generation required to sensor operate and start the scanning process and transmition data to computer. The SPR sensor Spreeta output is coupled to an A/D converter with 16 bit resolution. The user interface was based on LabView framework, provides in real-time graphics associated with biosensor operations.

2. THEORY

2.1. Basic SPR Theory

Surface plasmons are longitudinal electromagnetic charge density oscillations that may exist at the metal-dielectric interface, under specific boundary conditions. With total internal reflection (TIR) and under energy and momentum conservation conditions, when a p-polarized light beam hits the metal surface, for a certain range of incidence angle, arises an evanescent electromagnetic field and the photons energy is absorbed by the surface plasmons. In that instant occurs a resonant interaction between evanescent electromagnetic field and surface plasmons oscillations, which is clear identified by a dip in the reflectance curve, as is depicted in Figure 2b and can be observed by a suitable light detector.

As new substances circulate through flow cell, they can settle in bio-recognition layer, changing the characteristics of sample in contact with metal surface (Fig. 2a). Such changes are characterized by a horizontal shift in the minimum amount of reflectance, ie, the angle or wavelength resonance.

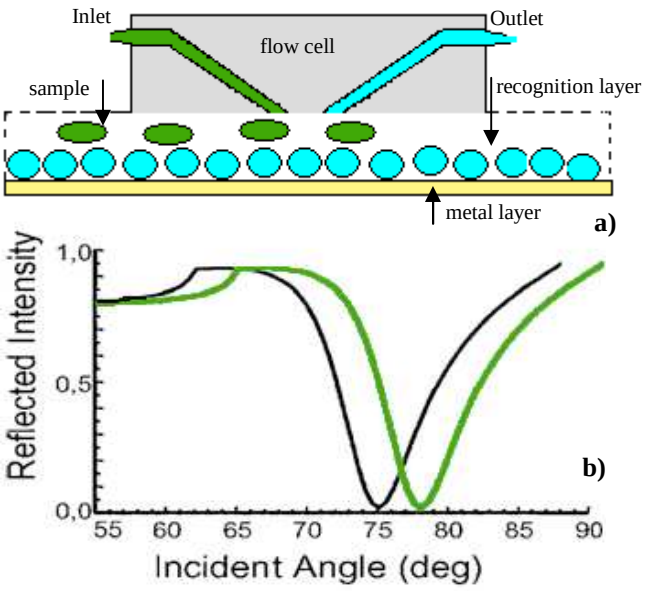

Fig. 2 a) when the new sample inlet, may bind to functionalized recognition layer resulting in b) horizontal shift in resonance angle

The behavior of a p-polarized light in a biosensor with multilayer structure (Fig. 1) is described in each environment by equations (1) e (2) [7]:

$$q_j = \frac{\sqrt{n_j^2 - (n_1 sen(\theta_j))^2}}{n_j^2} \quad (1)$$

$$\beta_j = \frac{2\pi}{\lambda} d_j \sqrt{n_j^2 - (n_1 sen(\theta_j))^2} \quad (2),$$

where $n_j = n_{jr} + n_{ji}$ é is the complex refractive index of the medium j; θ_j is the incidence angle of light that propagates in the middle j; d_j refers to width of layer and λ to wavelength of light-polarized.

Then, the light undergoes multiple reflections to penetrate into more remote layers and all must be taken into account in calculating of total reflection. However, there is an easier and convenient formulation in the literature to use to describe the transfer of a wave propagating through the medium j to $j+1$. Phys and Abelès apud [8] employ the so-called transfer matrix, given by equation (3):

$$M_j = \begin{bmatrix} \cos(\beta_j) & (-isen(\beta_j))/q_j \\ -iqsen(\beta_j) & \cos(\beta_j) \end{bmatrix} \quad (3)$$

Thus, the total transfer can be calculated as a function of transfer matrix (3) for each interface between medium, generating a total transfer matrix (4):

$$M_{tot} = M_2 M_3 \dots M_{m-1} = \prod_{i=1}^{m-1} M_i = \begin{bmatrix} m_{11} & m_{12} \\ m_{21} & m_{22} \end{bmatrix} \quad (4)$$

Finally, using equation (1) and the total transfer matrix, equation (4), can calculate the reflectivity value (r) to system with m layers.

$$r = \frac{(m_{11} + m_{12} q_m) q_m - (m_{21} + m_{22}) q_m}{(m_{11} + m_{12} q_m) q_m + (m_{11} + m_{12}) q_m} \quad (5)$$

The changes in the bio-recognition layer, deposited on thin film of metal are expressed by this value, and are so-called as Fresnel coefficient.

3. SYSTEM DESCRIPTION

The proposed system can be seen in Figure. 3. All optical and electrical components are encapsulated in a single package, that corresponds to Spreeta. A SPR biosensor SPR exploits the plasmon resonance by adding a biochemical active layer on top of the thin metallic film thus creating a multilayer structure. Any changes in this layer are then captured and recorded in the sensor outputs. The parameters investigated on substances analysis may be the refractive index, concentration or mass of analyte, adsorption and dissociation chemical constant and generally available in graphs form by a computer.

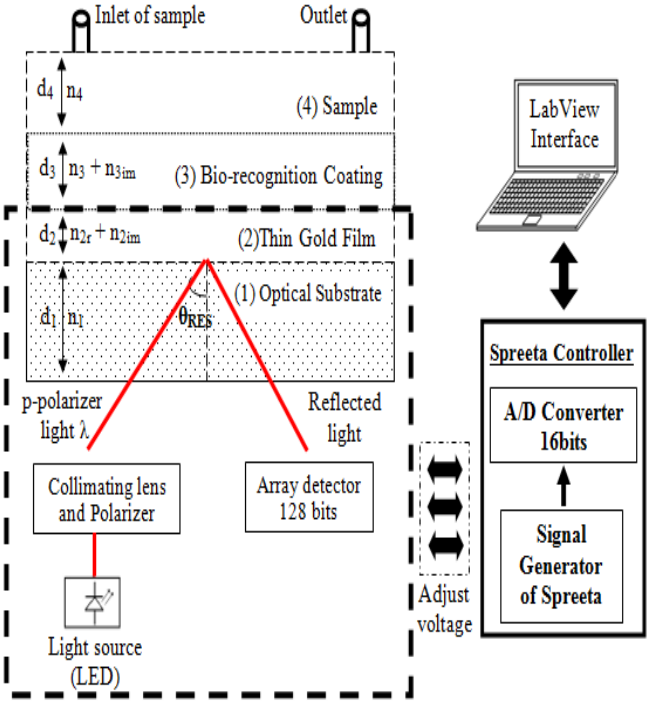

Fig. 3. System set-up showing all elements. Dotted line encompasses the Spreeta elements

Apply the appropriate signals at pins is necessary for measuring the refractive index of the liquid present at the sensing surface. Block diagram in Fig. 4 shows Spreeta pin assignments. The control unit generates in a coordinated manner clock, start, light source signals - responsible for exciting the SPR phenomenon - and transferring the sensor output to the computer. In Figure 4 see that the array

detector consists of 128 pixels, where each value is read sequentially. Every clock cycle a new pixel is available in the output.

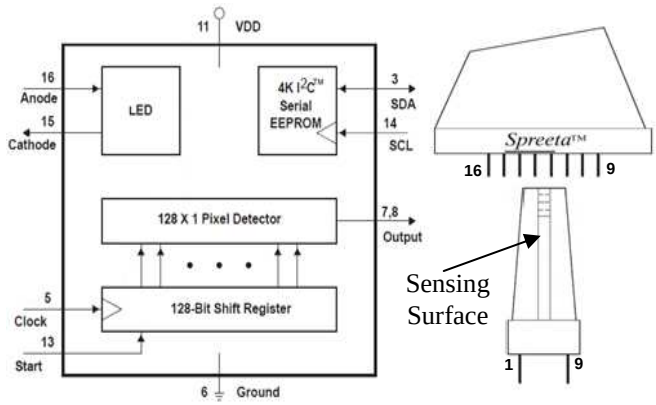

Fig. 4. (a) Spreeta block diagram and (b) physical structure

The pixels are captured by a CCD element (Charge Coupled Device) resulting in a trade-off between the light exposure time by CCD element (integration time) and LED intensity. The integration time determines the amount of light absorbed by the pixels in the array. A long period of light exposure causes a detector saturation (situation which one or more pixels are completely filled by excessive drainage of photons) introducing errors in the results. Thus the controller should be aware that: a) an increase in clock frequency causes a lower drainage of light, which implies higher values of voltage and current LED supplied; b) conversely a decrease in clock frequency causes greater light absorption resulting in low values of voltage and current for the LED. To find equilibrium, was fixed the integration period at same time it controlled the LED power by pulse width modulation. For the correct LED operation it should convey a 1.7V voltage in a 20mA current.

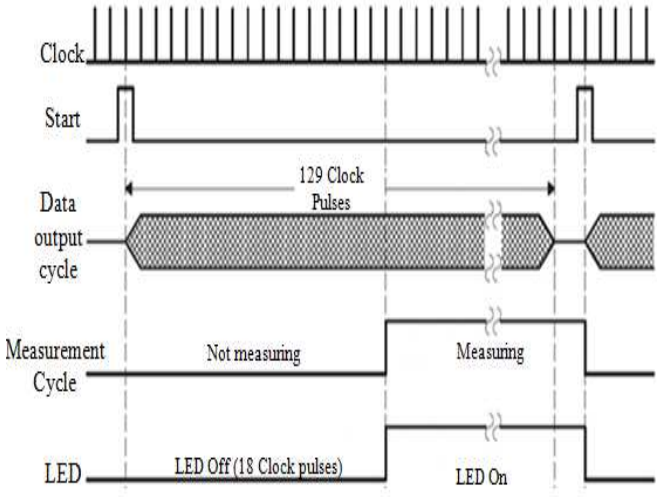

Fig. 5. Controller operation waveform

The controller operating cycle shown in Figure 5. To measure a refractive index, the LED must be illuminated during the measurement cycle, although not necessarily for the entire measurement cycle. In order to reduce energy consumption, the LED is kept off for 18 clock pulses, only connected minimum time allowed for the measurement cycle, that is 111 clock pulses. The integration period starts from the first Start signal rising edge. Simultaneously, the data output cycle begins and the first data bit is presented to the output pin. The end of the integration period is in 129th clock pulse. The measurement cycle requires an extra pulse (129th) end the acquiring cycle and clean the internal shift register [9]. The measurement cycle continues until the next start pulse is clocked into the internal shift register.

The output data consists of 128 bits of analog data from a charge mode linear array detector. For each bit the output voltage is a product of measurement time and LED illumination. The output voltage of each bit has a range of 100 mV (when the LED is off and the sensor is in a completely dark environment) to 3V. The measurement cycle should be adjusted so that the average output voltage level of all 128 bits is 2.5 V with the LED illuminated the sensor in a dark environment, and with no liquid on the sensing surface. [10].

The response provided by Spreeta is subject to various noise sources, many of them intrinsic of sensor design. One of most effective ways to minimize this problem is the A/D converter choice. With 8 bits resolution the noise level is about $3.0 \times e^{-6}$ RIU (Refractive Index Unit) [10]. This work used a 16 bits resolution resulting a noise level approximately $1.125 \times e^{-6}$ RIU (37.5% less).

3.1. Hardware implementation

As seen, only the correct signaling are capable of controlling Spreeta operation. Given this, a dedicated IP core was designed to providing the sensor signals. For signal generation a core processor and registers banks are not necessary, minimizing energy consumption. Another consequence is the flow design simplicity for microfabrication. Possessing a Small-Scale Integration level (SSI) containing 45 logic elements, creates a floorplanning suitable for extreme ultraviolet lithography of 13nm [11], which drastically reduces the amount of silicon needed for chip manufacture.

In Figure 6 are controller modules. The clock frequency varies between 25 kHz and 2 MHz. At these frequencies Spreeta output updates approximately at 300ns. Start pulse is coordinated with clock generator, synchronizing data acquisition process. It is important that the start pulse go low before the second clock pulse in the data output cycle. Having more than one start pulse in the internal shift register is an illegal condition [10]. Moreover, the Start signal triggers the start conversion by analog-to-digital converter.

The LED controller operates at 50% duty cycle (PWM signal), enough to provide 1.7 V specified by the sensor datasheet, under 3.3V FPGA outputs which the controller was prototyped.

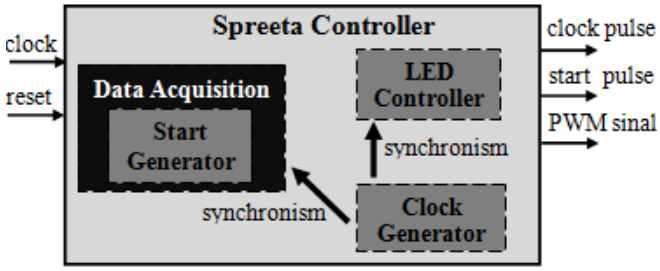

Fig. 6. IP core block diagram

3.2. Software implementation

The software implements data acquisition and data manipulation algorithms of Spreeta and makes them available in a graphical user interface, see Figure 9. To maintain real-time monitoring, the data from Spreeta must be read in a continuous update process. Given this situation, the data precision was conditioned to three decimal places resulting in a faster screen refresh.

The refractive index range which sensor can detect goes from 1.320 to 1.368 RIU, resolution varies depending upon the A/D converter (starting from 12 bits resolution) and algorithm used. The determination of resonance occurrence is given by calculating polynomial fit of SPR curve. This adjustment consists in approximate SPR curve, or region near to minimum of curve, to one polynomial of n degree type $P_n = a_0 + a_1 x + \cdots + a_n x^n$.

Given the set of sensor pixels, denoted by $X(n) = \{x_1, x_2, \ldots, x_{128}\}$ the algorithm find a polynomial such that $P_n \cong X(n)$. The wavelength or angle of resonant is then calculated by minimizing the value of polynomial obtained.

Owing to visual programming versatility, software data acquisition flow divided into real time tasks, time-critical tasks and offline tasks (see Figure 7). Real time tasks are defined by the sensor hardware, through integration time for data provision for A/D converter and from the detector array. The critical-time tasks are defined through continuous operations of updating data on screen and user parameters. And so-called off-line tasks refer to disk storage.

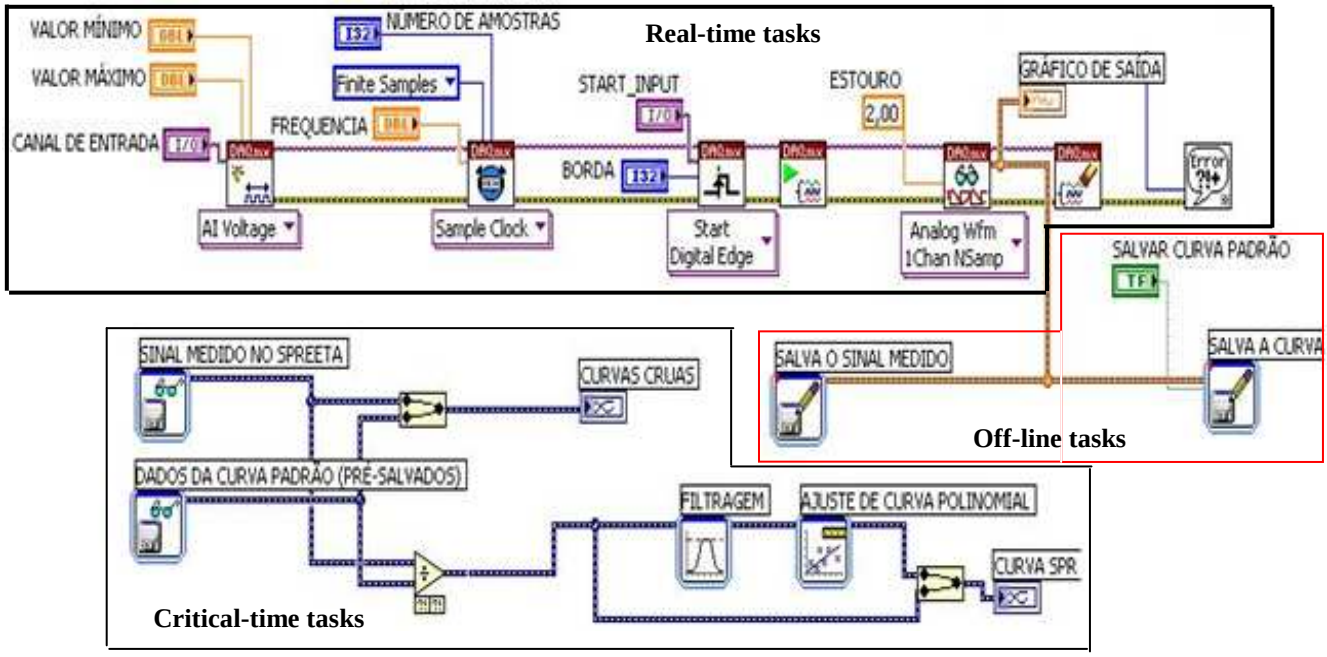

Fig. 7 Software design within Labview. Highlight for different tasks types.

.

4. EXPERIMENTS AND RESULTS

4.1. Experimental Design

In order to illustrate a practical application of proposed IP core, an experiment to determinate the resonant angle for different substances was performed. The experiment consists in acquire a reference signal for sensor calibrate and then continuously monitors the substances refractive index passing over the sensitive gold surface.

The experimental set-up can be visualized in Figure 8. Into a controlled lighting ambient, the resonance moment observed for degassed and deionized water (H_2O), sodium hydroxide (NaOH) at 0.2 molar concentrations, Ethanol in a 5% concentration solution and to Hypochlorite.

Owing to analog nature of the system a power supplied completely isolated from the A/D converter minimizes the electrical noise, maximizes the sensitivity of Spreeta output.

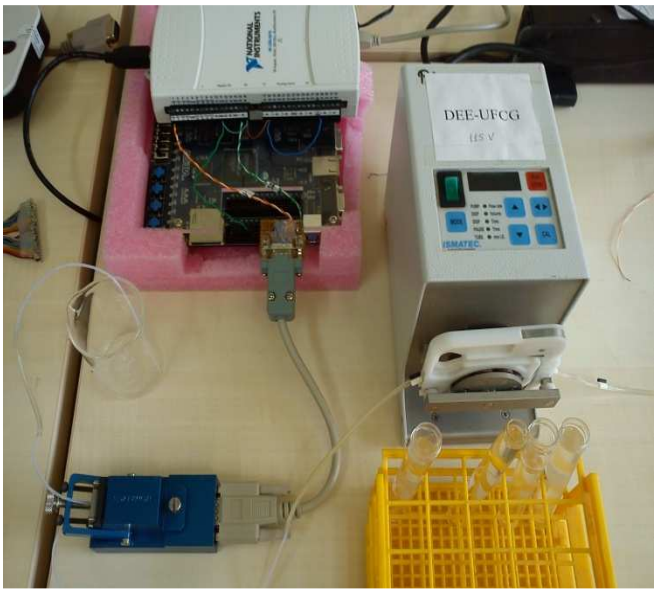

Fig. 8. Set-up experimental.

Taking air as reference signal, $X(n)_{Air}$ (Figure 9b blue line), estimated the SPR curve signal (Figure 9c) dividing the current $Y(n)$ (Figure 9a) by reference, as equation (6):

$$SPR(n) = \frac{Y(n)}{X(n)_{Air}} \quad (6)$$

4.2. Results and discussion

The resonance angles obtained are in Table 1.

Table 1 Sensor response. Resonance angle for different substances

Resonance angle (degree)	Substances			
	Hypo.	H_2O	NaOH	Ethanol
Exp. 1	72.570	68.000	69.958	68.313
Exp. 2	72.663	68.003	69.801	68.891
Exp. 3	73.004	67.999	69.777	68.663
Average	72.75	68.00	69.85	68.62
Standart deviation	0.22	0.24	0.10	0.3

The biosensor calibration followed the guidelines outlined in [10]. The resonance moment for water occurred in the 93rd pixel of array detector. As the resonant angle for water is knew, obtained a linear relationship between the pixel with lower intensity and resonance angle, expressed by (7):

$$\theta(x) = -0.354x + 100.55 \quad (7)$$

The results obtained for resonant angles (Figure 9d) were compared with Fresnel equations analytic solution simulated by computer (H2O = 67.92, NaOH = 69.89, Ethanol = 68.56 e Hyp. = 72.6), revealing errors percentage of 0.26%, 0.23%, 0.22% e 0.36% for H2O, NaOH, Etanol e Hypochlorite respectively. These data attests the correct functioning of sensor, and therefore the correct signals applied by the proposed controller.

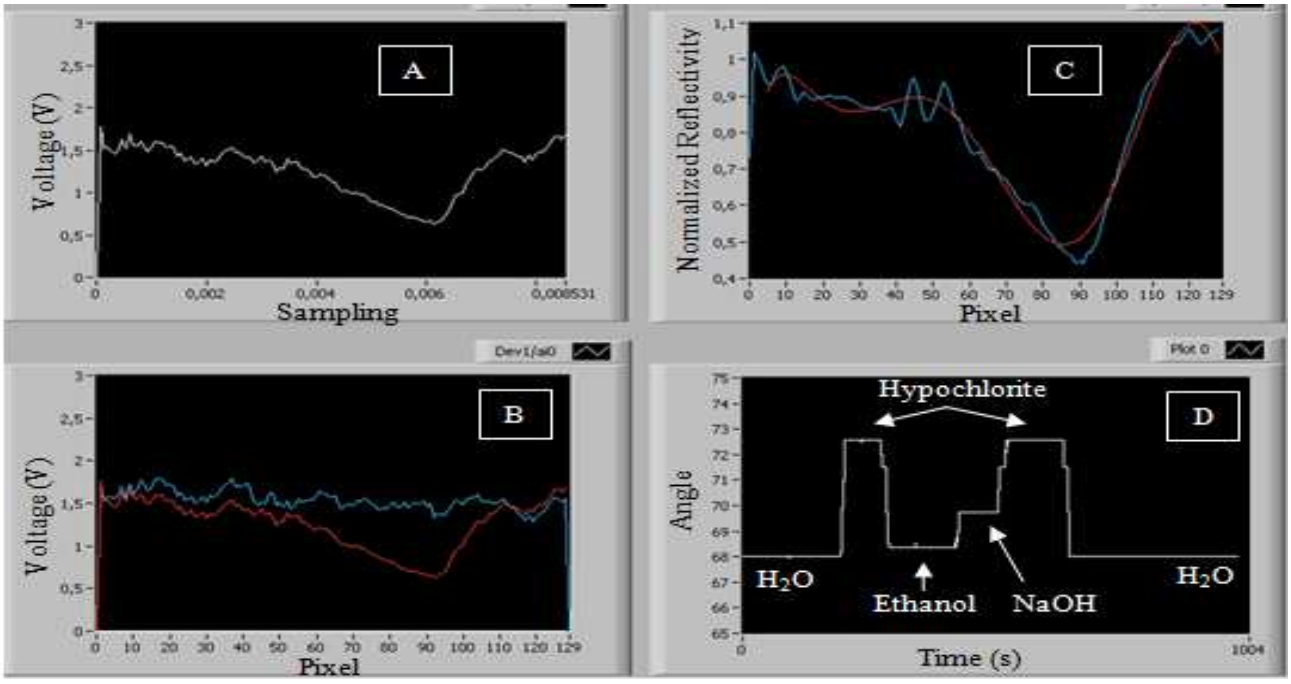

Fig. 9 Software interface showing a)current signal b) reference signal (blue) and current signal (red) c) SPR curve (blue) and polynomial approximate (red) and d) sensorgram (resonance angle *versus* time).

4. CONCLUSIONS

A controller chip dedicated to providing the control signals for Spreeta SPR sensor was prototyped. Its use minimize the need of external hardware, providing greater system reliability. The experiments are good examples of our project ability. Due a simple architecture, 13nm microfabrication technology may be implemented. Integrated with the sensor Spreeta provides a good alternative for systems analysis at low cost.

AKNOWLEDMENTS

Financial support and research grant by CNPQ is gratefully acknowledged.

REFERENCES

[1] H. Neff, T. Beeby, A. M. N. Lima, M. Borre, C. Thirstrip, W. Zong and L. A. L. de Almeida. *Dc-Sheet resistance as sensitive monitoring tool of protein immobilization on thin metal films. Biosensors and Bioelectronics*. **21**, 9, p. 1746-1752. (2006)

[2] M. Pohank, P. Skládal and M. Kroèa. *Biosensor for Biological Warfare Agent Detection. Defense Science Journal*. **57**, p. 185-193. (2007)

[3] N. V. Zayteseva, R. A. Montgana, E. M. Lee, A. J. Baeumner. *Multi-analyte single-menbrane biosensor for the serotype-specific detection of Dengue virus. Bional Chemistry*, **380**, p. 46-53. (2004)

[4] G.C.A.M. Bokken, R. J. Corbee , F. van Knapen and A.A. Bergwerff. *Immunochemical detection of Salmonella group B, D and E using a optical surface plasmon resonance biosensor*. *Microbiology Letters*, **222**, p. 75-82 (2006)

[5] J. Homola, S.S Yee and G. Gauglitz. *Surface plasmon resonance sensor: review. Sensors and Actuators B.* **55** (1999)

[6] National Direct Network "SPR Evaluation Kit" website: http://ndn.co.th/products%20index/Instrument%20biosensor.html

[7] Neff, H.; Zong, W.; Lima, A.M.N.; Borre, M.; Holzhüeter, G. *Optical properties and instrumental performance of thin gold films near the surface plasmon resonance*. *Thin solid Films*, v. 496, p. 688–697, October 2006

[8] Thistrup, C.; Zong, W.; Borre, M.; Neff, H.; Pedersen, H.C.; Holzhüeter, G. *Diffractive optical coupling element for surface plasmon resonance sensors. Sensors Actuators B:Chemical*, v. 100, n. 3, p. 298–308, Mai 2004.

[9] Texas Instrument, *Analytical Sensor SPREETA Datasheet*. (2000)

[10] Texas Instrument, Technical Notes: *The binding of neutravidin followed by the attachment of biotinylated antibodies to the Spreeta surface.* (1999)

[11] R. C. Jaeger. *Introduction to Microelectronic Fabrication*. Second Edition. p. 1-40. Prentice Hall, New Jersey. (2002)